Macromolecules 1984, *17*, 2520–2529

Coagulative Nucleation and Particle Size Distributions in Emulsion Polymerization

P. John Feeney, Donald H. Napper, and Robert G. Gilbert*

Departments of Physical and Theoretical Chemistry, University of Sydney, Sydney, N.S.W. 2006, Australia. *Received November 14, 1983*

ABSTRACT: A detailed theory is presented for nucleation kinetics in emulsion polymerization systems based on the coagulation of precursor particles (which may themselves be formed by either homogeneous nucleation or micellar entry). These precursor particles differ from true latex particles by a slower rate of polymerization and the lack of stability against coagulation. The coagulative nucleation theory combines extended Müller–Smoluchowski coagulation kinetics with DLVO theory. Expressions are provided for the time evolutions of the nucleation rate, particle number, and particle size distribution (PSD). With physically reasonable values for the parameters for the coagulation kinetics, agreement is obtained with data for styrene emulsion polymerization systems. In particular, excellent accord is obtained with the early-time evolution of the PSD, such data being especially sensitive to assumptions as to the nucleation mechanism. In addition, agreement is obtained with data on the dependence of particle number on surfactant and initiator concentrations.

Introduction

A number of mechanisms have been proposed for latex particle formation in emulsion polymerization systems.[1,2] These include primary particle formation by entry of a free radical into a micelle[3] or by homogeneous nucleation of oligomeric free radicals in the aqueous phase[4] or (if appropriate additives are present) within microdroplets of the monomeric emulsion.[5] After their formation, these primary particles may simply grow by conversion of monomer to polymer within these particles or undergo coagulation, as has been suggested by a number of authors.[6-9] In the present paper, it will be shown that there is strong experimental evidence for nucleation indeed being a coagulative process, and the appropriate theory for describing this will be derived.

A major problem in deciding which mechanism(s) is (are) applicable to a given monomer under a particular set of conditions is that experimental data are often consistent with more than one mechanism. For example, while Smith and Ewart[10] showed that the micellar entry mechanism can lead to the particle number density and thus the polymerization rate being proportional to $[I]^{0.4}[S]^{0.6}$ (where [I] is the initiator concentration and [S] the surfactant concentration), it was later shown by Roe[11] that this behavior is also consistent with homogeneous nucleation. It has recently been demonstrated[12] that a more sensitive test of the theories describing the nucleation mechanism in an emulsion polymerization system is provided by the determination of the time evolution of the full particle size distribution (PSD) of the latex sometime after the cessation of nucleation. It was shown that, for a persulfate-initiated styrene emulsion polymerization using sodium dodecyl sulfate as surfactant, the early-time PSD plotted as a function of the particle volume was positively skewed. This implied that the rate of production of new latex particles must have been an increasing function of time for much of the nucleation period, although the rate ultimately must have dropped off quite rapidly near the completion of nucleation. Any one-step micellar entry or homogeneous nucleation mechanism could not have been operative in this system because both mechanisms predict that the rate of production of new latex particles decreases monotonically with time or at least remains constant.[12]

The observation that the rate of production of latex particles increases during much of the nucleation period was explained by Lichti et al.[12] in terms of a two-step coagulative nucleation model. In this, the first-formed "precursor particles" undergo coagulation to form "true" (i.e., mature) latex particles. The term "precursor particle" is used here to designate a primordial latex particle formed by the polymerization of a single (or at most, a few) free radical species, either in the aqueous phase (leading to homogeneous nucleation) or, possibly, after entry into a micelle. Such particles differ from mature latex particles in at least two important respects: first, they are colloidally unstable, undergoing coagulation with other precursor particles or with mature latex particles; second, they polymerize very slowly. The ultimate justification for these assumed differences must reside in their ability to predict correctly the time evolution of the PSD of the formed latexes. Nevertheless, these assumptions do have plausible physical bases. First, the colloidal instability of precursor particles may be presumed to arise from their small size and the concomitant curvature of their electrical double layers; calculations in this paper using DLVO theory confirm that, for particles whose size is less than a few nanometers, it is often not feasible to impart the relatively high surface charge densities required to generate robust colloid stability. Second, the slow rate of polymerization of precursor particles may arise from (i) the reduced swelling of the particles by monomer, due to their hydrophilic character[12] and/or their small particle size,[13] and (ii) rapid exit of any free radicals in the precursor particles arising from their small size.[14] The precursor particles are presumed to grow mainly by coagulation, although some growth must occur by polymerization.

In the above discussion, for simplicity all particles are assumed to belong to one of two categories: unstable precursor particles and stable latex particles. In fact, as will be explicitly shown in a later section, particles show an entire spectrum of colloidal stability, and the quantitative model presented later in this paper takes this gradation of stability fully into account. It is however convenient for qualitative purposes to label as "precursor" those particles whose lifetime for coagulation (either with themselves or with true latex particles) is less than the nucleation period, and as "latex" particles those whose lifetime is greater than this period.

It is stressed that a unique and essential feature of the coagulative nucleation mechanism is that precursor particles be qualitatively different from mature latex particles in both their polymerization rate and colloid stability. In this, they differ from the primary particles alluded to above which are postulated to possess the properties of mature latex particles. Nucleation models invoking such primary particles, even if these undergo coagulation, are quite

0024-9297/84/2217-2520$01.50/0

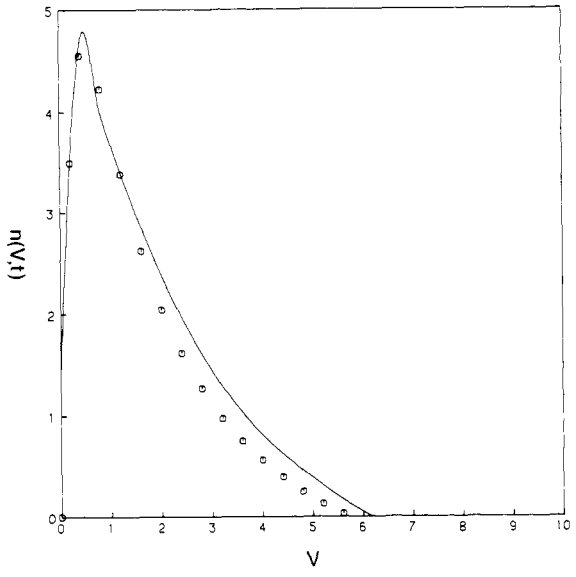

Figure 1. PSD, $n(V,t)$ [arbitrary units], as a function of volume, V (10^4 nm^3), computed from dN_c/dt of Figure 7 (full line) compared with experimental data (points) at $t = 8$ min; experimental details in text.

unable to explain the observed increase in nucleation rate with time and so will not be considered further. It is further stressed that the precise nature of the size and chemical composition of precursor particles is not crucial to the general conclusions of the theory presented below. Note that it is not possible to exclude the micellar entry nucleation mechanism if the particles so formed polymerize only slowly and subsequently undergo coagulation. The former seems unlikely, however, in view of the amount of monomer solubilized within the micelles and the latter scarcely seems consistent with the large amount of surfactant that would be associated with particles produced by such a mechanism.

It is useful to consider in more detail how PSD data can be used to suggest a coagulative nucleation mechanism. The PSD at early times is plotted as a function of the unswollen volume V (rather than as a function of radius or some other size variable); V is the "natural" variable in which to express a PSD, since a polymerizing particle changes its unswollen volume uniformly in time. Early-time PSDs, in terms of V, are almost invariably positively skewed (see, e.g., Figure 1): most particles have comparatively small volumes. This implies that most particles are formed comparatively late in the nucleation period and so have not grown very much (unless the kinetic parameters for propagation, entry, and exit showed a dependence on particle size that would be however counter to both expectation and experiment). Thus the nucleation rate must be an increasing function of time. Now, micellar entry *alone* or homogeneous nucleation *alone* would give nucleation rates which are nonincreasing functions of time. The coagulative nucleation mechanism explains the increasing rate of production of latex particles by an increase in the number concentration of precursor particles which grow mainly by undergoing coagulation to form true latex particles.

Two points are worthy of note here. First, a positively skewed PSD could also be obtained from kinetics wherein free radical entry and/or particle growth were very strong functions of particle volume; however, the required volume dependences are physically unreasonable. Second, the positive skewness upon which the argument is based is only observed at early times, since "stochastic broadening" (caused by free radicals entering into, exiting from, and mutually terminating within latex particles) causes any PSD to lose skewness sufficiently long after nucleation has ceased.

Both the qualitative results of a maximum in the particle number as a function of time and the positively skewed early-time PSD (as well as a more detailed quantitative interpretation) provide compelling evidence that particle formation involves a coagulation step: precursor particles which polymerize only slowly are formed by homogeneous nucleation or by micellar entry and then subsequently undergo coagulation to form true latex particles. The present paper develops theory and data reduction methods for a coagulative nucleation mechanism. First, a quantitative formulation of the coagulation kinetics of precursor particles is presented based on an extension of simple Smoluchowski-type coagulation theories[15-17] together with DLVO theory.[18] This gives the expected time-increasing coagulation rate (and replaces the empirical expression for this rate used by Lichti et al.[12]). Second, with this result, an analytic expression for the time evolution of the PSD is obtained (replacing the numerical solutions of Lichti et al.[12]). The interpretation of data using these results yields agreement with the qualitative arguments used above and which are also in good accord with the Smoluchowski-type model.

Theory of Coagulative Nucleation

In the standard Smoluchowski theory of rapid coagulation,[15,16] one considers the flocculation kinetics of a system in which an initially homogeneous dispersion of monodisperse primary particles undergoes coagulation, with no new particles being introduced. However, for the coagulative nucleation kinetics of an emulsion polymerization system, there are initially no particles present, and precursor particles of the type described above are formed continuously during the nucleation period. This feature can be readily incorporated into the basic model. In the following, two developments of the coagulative nucleation kinetics are presented: (i) a direct extension of the simple Smoluchowski theory, yielding an analytic solution to the time dependence of the nucleation rate, which is qualitatively correct but which does not give good quantitative agreement with experiment, and (ii) a more complete treatment which yields equations which can only be solved numerically but which compares quantitatively with experiment.

(i) Simple Smoluchowski Theory. Let v_i, $i = 1, 2, 3, \ldots$, be the number of i-fold particles formed by the flocculation of precursor particles. Precursor particles are denoted by $i = 1$. Note that a precursor particle will consist of one or more polymer chains of comparatively high degree of polymerization. The precursor particle may be formed by micellar entry, homogeneous nucleation, or entry into microdroplets; let the rate of formation of these precursor particles be $g(t)$. The entities formed by coagulation of a total of i of these precursor particles have concentrations v_i. Since k-fold entity is formed by coagulation of an i-fold and a j-fold, with $k = i + j$, one has on extending the Smoluchowski model[15,16] an expression for the rate of coagulation:

$$\frac{dv_k}{dt} = \frac{4\pi DR}{W}\left[\sum_{i=1}^{k-1} v_i v_{k-i} - 2v_k \sum_{i=1}^{\infty} v_i\right] + \delta_{k,1} g(t) \qquad (1)$$

Here, $\delta_{k,1} = 0$ for $k \neq 1$, $\delta_{k,1} = 1$ for $k = 1$, D is the diffusion coefficient of a precursor particle whose radius is $R/2$, and W is the stability ratio. The last named is the reciprocal of the probability that an encounter between two particles (precursor or otherwise) will result in coagulation. The

term $4\pi DR/W$ is referred to as the Smoluchowski rate coefficient for particle coagulation.

The major assumptions involved in eq 1 are inter alia that coagulation is entirely diffusion controlled and that the product of the mutual diffusion coefficient and the mutual radius of interaction between an i-fold floc and a j-fold floc may be approximated by DR. Furthermore, all coagulation events are assumed to occur at the same rate, regardless of the radii of the coagulating species.

To obtain the total number of particles, eq 1 is summed over all k, giving

$$dv/dt = g(t) - 4\pi DRv^2/W, \qquad v = \sum_{k=1}^{\infty} v_k \tag{2}$$

We now assume pro tem. that $g(t)$ is time independent during the nucleation period (this restriction will be relaxed to some extent at a later stage). Equation 2 can then be integrated subject to the appropriate boundary conditions [$v_i(t = 0) = 0$ for all i] to yield

$$v = C \tanh (Bt/2)$$

where

$$B = 4\left(\frac{\pi DRg}{W}\right)^{1/2}, \qquad C = \left(\frac{Wg}{4\pi DR}\right)^{1/2} \tag{3}$$

Equation 1 can be similarly solved for $k = 1$, giving

$$v_1 = \frac{g}{B}\frac{\sinh (Bt) + Bt}{\cosh (Bt) + 1} \tag{4}$$

If we now suppose that latex particles contain two or more precursor particles (this could obviously be extended to any higher degree of coagulation if necessary), then the number of latex particles, N_c, is given by

$$N_c = v - v_1 = C \tanh\left(\frac{Bt}{2}\right) - \frac{g}{B}\frac{\sinh (Bt) + Bt}{\cosh (Bt) + 1} \tag{5}$$

The value of the particle number at infinite time is given by

$$N_c(t = \infty) = C - g/B \tag{6}$$

An estimate of the values of the parameters required to calculate N_c from eq 6 can be made for a typical system[8] as follows. The rate of production of precursor particles, g, is estimated as being that of the rate of decomposition of 10^{-3} mol dm^{-3} $K_2S_2O_8$ at 50 °C (the conditions of Lichti et al.[12]), yielding $g \sim 10^{15}$ particles dm^{-3} s^{-1}. One notes that much more sophisticated means of estimating g have been developed (inter alia by Fitch and co-workers[8,19]) but the value of 10^{15} dm^{-3} s^{-1} suffices for the present order-of-magnitude requirement. DR is calculated from the Stokes–Einstein relation, $DR = k_BT/6\pi\eta$ (where T is the temperature, k_B is the Boltzmann constant, and η the viscosity of the aqueous medium). The value of the stability ratio W is then estimated from eq 6 by setting the final ($t = \infty$) value of N_c to the experimental value of 10^{17} particles dm^{-3}. This yields $W \sim 4 \times 10^5$. The comparison of this value with that expected from stability theory will be made later.

Figure 2 shows the nucleation rate dN_c/dt as a function of time, obtained with the above parameters and the differential of eq 5. The curve shows features which are qualitatively in accord with experiment (see Figure 7 and ref 8): principally dN_c/dt is an increasing function of t at the commencement of nucleation. Note also that dN_c/dt shows a maximum during the nucleation period.

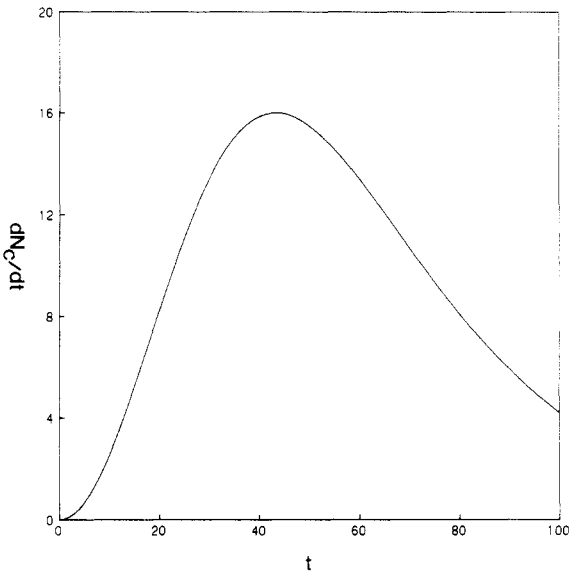

Figure 2. Nucleation rate, dN_c/dt (particles/10^{-10} dm^3 s^{-1}), as a function of time, t (s), from simple Smoluchowski theory, eq 5, using parameters given in the text.

Although the qualitative form of dN_c/dt predicted by eq 5 is in agreement with experiment, a quantitative comparison shows it is oversimplified. The experimental maximum rate is achieved near the end of nucleation,[12] at ca. 500 s, whereas the predicted maximum rate is at a considerably shorter time, ca. 40 s. In addition, the value of W obtained by fitting to the experimental $N_c(t = \infty)$, 4×10^5, although reasonable for latex particle/latex particle interactions, is too large for precursor/precursor collisions (see below). If W is reduced by an order of magnitude, then the maximum in dN_c/dt is reached at ca. 20 s, which is in even greater conflict with experiment. To obtain agreement with the observed maximum in dN_c/dt, the stability ratio needs to be 10^7–10^8, which is physically unreasonable.

An obvious failing of the simple Smoluchowski model is that it assumes that W is independent of the degree of coagulation of the flocculating particles: one would expect W to be smaller for small particle/small particle interactions than for large particle/large particle interactions. In addition, no account is taken of what happens when particles grow to an extent that 100% coverage by surfactant is no longer possible. It is now shown that removing these restrictions results in a model which agrees quantitatively with experiment.

(ii) Modified Coagulation Theory. In order to resolve this discrepancy, the extended Smoluchowski mechanism can be modified by using the Müller theory for coagulation.[17] The Smoluchowski rate of particle interaction, $4\pi DR/W$, is replaced by the Müller rate, B_{ij}, where

$$B_{ij} = \frac{4}{3}\frac{k_BT}{\eta W_{ij}}\frac{(1 + r_i/r_j)^2}{4r_i/r_j} \tag{7}$$

Here, B_{ij} refers to the rate of coagulation between an i-fold and a j-fold flocculated particle. W_{ij} is the stability ratio of the i-fold and the j-fold particles and r_i and r_j refer to their radii. The rate of coagulation of differently sized particles may now be faster than the rate for similar sized particles. Equation 1 can now be modified to give the following equation:

$$dv_k/dt = \sum_{i=1}^{k-1} B_{i,k-i}v_iv_{k-i} - 2v_k\sum_{i=1}^{m} B_{k,i}v_i - 2v_kB_{N,k}N_c + \delta_{k,1}g(t) \tag{8}$$

$$dN_c/dt = \sum_{i=1}^{m} v_i \left(\sum_{j=m-i+1}^{m} B_{ij} v_j \right) \quad (9)$$

Here, $m + 1$ is the number of coagulated precursor particles in the smallest entity which is a true latex particle, these being assumed stable to self-coagulation, but which coagulate with other particles with rate $B_{N,k}$. The particles have thus been partitioned into three classes: precursors ($k = 1$) and higher flocs ($k = 2, ..., m$) which can coagulate both with each other and with the latex particles, and latex particles ($k > m$) which cannot undergo homocoagulation ($W_{kj} = \infty$, $k > m, j > m$) but may coagulate with precursor particles. Thus it is assumed that precursors and other particles coagulate until the particle so obtained has acquired a critical number ($m + 1$) whereupon they become stable latex particles; i.e., there is a critical particle radius. Note that this model ignores any growth by polymerization (other than by coagulation). This approximation is reasonable if the polymerization rate is low within the particles (because of low swelling and high exit rate). Note that adsorption of oligomeric free radicals is incorporated through the terms in v_1.

Before proceeding to discuss the new model further, it must be pointed out that it now includes more parameters than were present in the simple Smoluchowski theory, viz., the value of m, the r_i, and the parameters and form of W_{ij}. Because the choice of these parameters must perforce be subject to some latitude, this improved model cannot be quantitatively predictive, unless these values can be obtained by independent experiments. However, if data can be fitted with these parameters in a physically acceptable range, one can legitimately claim that it provides a realistic description of the nucleation process.

The stability ratio can be estimated from the relation[16]

$$W_{ij} = (\kappa r_{ij})^{-1} \exp(E_m/k_B T), \quad r_{ij} = 2r_i r_j/(r_i + r_j) \quad (10)$$

where κ^{-1} is the thickness of the double layer[20] and E_m the height of energy barrier to coagulation. The value of E_m can be obtained from DLVO theory[18] as the maximum in the interparticle potential function $V = V_R + V_A$, where the repulsive potential V_R is given by

$$V_R = \epsilon r_{ij} \psi_0^2 \exp[(-\kappa r_{ij})(s - 2)]/s \quad (11)$$

and the attractive potential V_A by

$$V_A = -\frac{A}{6}\left[\frac{2}{s^2 - 4} + \frac{2}{s^2} + \ln\left(\frac{s^2 - 4}{s^2} \right) \right] \quad (12)$$

Here, $s = 2 + (H/r_{ij})$, H is the distance of closest approach of the surfaces of the particles, ψ_0 is their surface potential, and A is the effective Hamaker constant of the latex particles in the dispersion medium.

Estimates of stability ratios for latex particles in a number of emulsion polymerization systems have been carried out for several systems[18,21] using DLVO theory. We use here the same methodology to estimate W_{ij} for a typical precursor/precursor interaction (W_{11}) as follows. The surface potential ψ_0 can be approximated by the ζ potential.[22] Now, this potential for small (coagulatively unstable) particles is difficult to measure or estimate. As a guide, a measurement was carried out of the ζ potential of styrene latex particles of unswollen radius 28 nm, prepared by the method of Hawkett et al.,[23] at the same temperature and similar surfactant concentration as used for the data of Figure 1. This yielded an apparent ζ potential of $\gtrsim$300 mV for the latex in 10^{-2} mol dm^{-3} sodium dodecyl sulfate. The precursor particles, although much smaller than these 28-nm particles, might be expected to have a comparable (but possibly smaller) ζ potential; a value of 200 mV (which will be seen to give agreement with experimental rates) is thus a reasonable estimate for ψ_0. A reasonable value for r_1 is 4 nm, this being the swollen radius of a styrene particle of 60% weight fraction polymer (being twice the weight fraction in a fully swollen particle at the start of interval II) containing a single chain of molecular weight 10^5 (there is experimental evidence[24] that this is an appropriate value for the molecular weight of polymer in coagulating precursor particles in styrene emulsion polymerization systems at 50 °C). With $A = 5 \times 10^{-21}$ J[18] and $\kappa = 3.29 \times 10^8$ m^{-1}[25] (as appropriate to a 5×10^{-3} mol dm^{-3} solution of sodium dodecyl sulfate, this concentration being the cmc at 50 °C), the potential curves calculated for a range of values of s using eq 11 and 12 are shown in Figure 3.

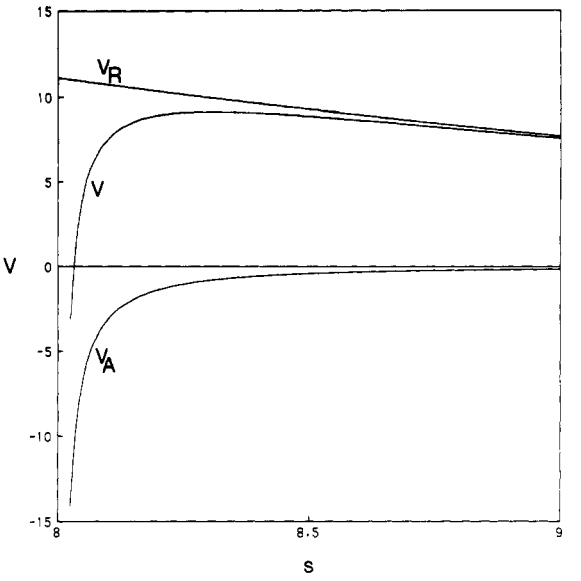

Figure 3. Attractive and repulsive potentials, V_A and V_R, respectively, and $V = V_A + V_R$ (units of $k_B T$) as functions of interparticle distance, s (nm), from eq 11 and 12, using parameters in the text.

From Figure 3, it is seen that the maximum energy barrier, $E_m \simeq 9.2 k_B T$, is found for $r_{11} = 8.3$ nm. From eq 10, this gives $W_{11} \sim 7 \times 10^3$. Carrying out the same calculation with $r_1 = 2$ nm and $\psi_0 = 300$ mV yields $W_{11} \sim 7 \times 10^4$. These calculations provide an estimate of the stability ratio for precursor/precursor particle interactions. Although it must be acknowledged that the DLVO assumptions are not likely to be quantitatively valid when applied to such small particles, one would expect eq 10–12 to provide valid orders of magnitude and trends (e.g., for the variation with particle size).

Having carried out a preliminary estimate of W_{11}, we now derive expressions for W_{ij} and B_{ij} between any i- and j-fold coagulated precursors (flocs) using eq 7 and 10–12. We assume that all flocs are spherically symmetric, and thus $r_i = i^{1/3} r_1$. We must next determine the variation of E_m with i. Figure 3 shows that for small values of r_{ij} (which is certainly the case for the systems considered here), E_m is dominated by the value of V_R, the repulsive component to the total potential. From eq 11 and Figure 3 one has V_R is approximately proportional to the interparticle distance $r_{ij} = r_i + r_j$, and thus so is E_m. Thus from eq 10

$$W_{ij} \propto r_{ij}^{-1} \exp(J r_{ij}) \quad (13)$$

where the coefficient J is determined from eq 10–12. Figure 4 shows a plot of $\ln (W_{ij} r_{ij}/W_{11} r_{11})$ against $(r_{ij} - r_{11})$ for the above values of the various parameters. From this plot, one obtains J ranging from 0.5 nm^{-1} ($\psi_0 = 100$ mV)

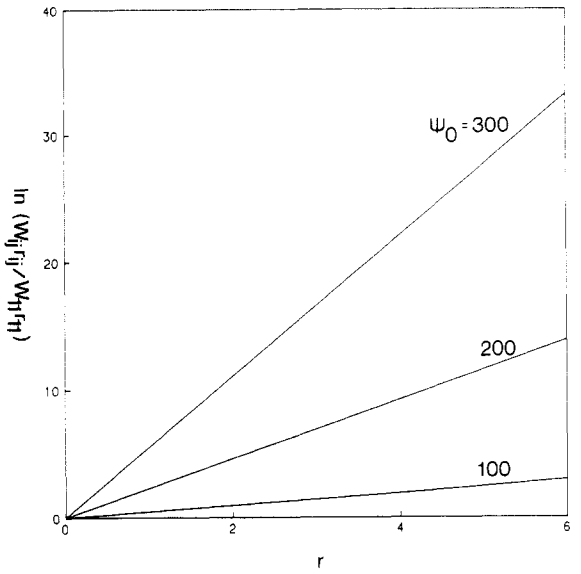

Figure 4. Ratio of logarithms of stability ratios multiplied by radius, ln ($W_{ij}r_{ij}/W_{11}r_{11}$), as a function of distance in radii, $r = r_{ij} - r_{11}$ (nm), from eq 14, for various values of ψ_0 (=100, 200, and 300 mV) and parameters in the text.

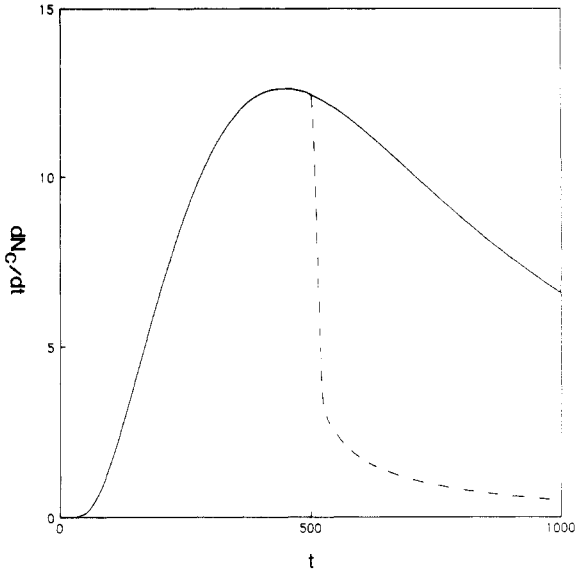

Figure 5. Nucleation rate, dN_c/dt (particles/10^{-14} dm^3 s^{-1}), as a function of time, t (s), from modified coagulation theory, eq 7–9 and 14–16, with $W_{11} = 8 \times 10^3$, $J = 2.0$ nm^{-1}, $r_{11} = 4.0$ nm, and $g = 10^{16}$ particles dm^{-3} s^{-1} and other parameters as given in the text. Full line: no account of surfactant exhaustion ($t_1 = \infty$); broken line: surfactant exhaustion incorporated from eq 16 (t_1 = 500 s).

to 5 nm (ψ_0 = 300 mV). This value was then adopted in the relation

$$W_{ij} = \frac{r_{11}}{r_{ij}} W_{11} \exp[J(r_{ij} - r_{11})] \qquad (14)$$

and the values of J and W_{11} treated as adjustable parameters in eq 7–9 and 14.

Figure 5 shows a typical curve (full line) for the time dependence of dN_c/dt with W_{11} and J values as indicated, computed by numerical solution of eq 7–9 with m (the value of the degree of coagulation above which true particles are deemed formed) taken as 10. This estimate is obtained by determining the smallest degree of coagulation of particles which are stable with respect to homocoagulation for the duration of the nucleation period (typically 10^2–10^3 s). The half-life with respect to homocoagulation of particles with initial concentration $v_j^{(0)}$ (obtained from solution of the equation $dv_j/dt = -B_{jj}v_j^2$) is $t_{1/2} = (1/2)/B_{jj}v_j^{(0)}$. With the above parameters, one finds that particles of degree of coagulation ~10 are stable for longer than the duration of nucleation.

It can be seen that (for physically reasonable values of J, W_{11}, and g, as estimated above) the time period over which dN_c/dt attains its maximum value is now in accord with experiment, viz. ca. 100–1000 s. However, it is seen also that the nucleation rate does not decrease sufficiently rapidly after the maximum to give an overall nucleation period in accord with the experiment. Selecting a lower value of m to counter this disagreement then gives the maximum in dN_c/dt at times that are then too short.

This apparent difficulty is readily overcome by incorporating an additional mechanistic feature whose importance is in fact well recognized: the alteration in surface properties when the surface area of the latex particles becomes sufficiently large that 100% coverage by the surfactant is no longer possible. This feature is specifically incorporated in the usual formulations of the micellar entry[10] and homogeneous nucleation mechanisms.[11] In the present formulation for coagulative nucleation, it is reasonable to assume that the formation of new precursor particles ceases at a time t, when there is no free surfactant to stabilize them, i.e., when the surfactant is exhausted. (Note that this feature will not be operative for systems below the cmc; while the general theory used here is applicable to such cases, the quantitative reliability of DLVO theory becomes suspect, and so such systems are not considered in the present paper). After surfactant exhaustion, the remaining particles coagulate until only latex particles remain; since coagulation is comparatively rapid, this will lead to a rapid decrease in dN_c/dt. One has

$$g(t) = g, \qquad t < t_1 \qquad (15a)$$

$$g(t) = 0, \qquad t > t_1 \qquad (15b)$$

The time t_1 can be estimated from the expression derived by Smith and Ewart[10] for the time when the total surface area of the particles equals that which can be covered by the surfactant. An important caveat here is that this assumes that each free radical generated by initiator decomposition leads to particle formation, an assumption which is questionable since there is ample evidence[23,26] that free radical capture efficiency after the cessation of nucleation is considerably less than 100%. Nevertheless, the Smith–Ewart formula should give a reasonable estimate for the order of magnitude of t_1. This formula is

$$t_1 = 0.65\left(\frac{a_S[S]}{K^{2/3}g}\right)^{3/5} \qquad (16)$$

Here, a_S is the area occupied by a surfactant molecule (e.g., ~0.6 nm^2 for sodium dodecyl sulfate), [S] is the surfactant concentration above the cmc, and K is the volume growth rate coefficient of a particle containing one free radical. Note that $K = k_p C_m M_0/N_A d_p$, where k_p is the propagation rate coefficient, C_m is the monomer concentration within the particles, M_0 is the molecular weight of monomer, N_A is Avogadro's constant, and d_p the density of polymer; $K^{2/3}$ is thus proportional to the rate of area growth per particle. One thus finds $t_1 \simeq 600$ s for 10^{-2} mol dm^{-3} sodium dodecyl sulfate with [I] = 10^{-3} mol dm^{-3} $K_2S_2O_8$.

The broken line in Figure 5 shows the effect on the nucleation kinetics of assuming that the rate of creation of precursor particles [$g(t)$] is zero for $t > t_1$, as in eq 15 and 16. The kinetics are of course the same as before for

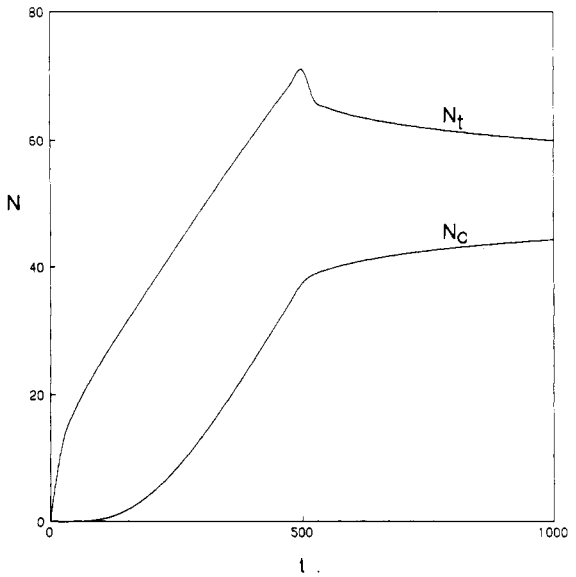

Figure 6. Particle number, N (particles/10^{-16} dm^3), as a function of time, t (s), from solution of eq 7–9 and 14–16, with parameters as given for Figure 5. N_c is the latex particle number; N_t is the total particle number.

$t \leq t_1$; thereafter dN_c/dt decreases rapidly to zero. This is now in accord with the experimental results for the time dependence of dN_c/dt from the time evolution of the PSD. Note also that the final particle numbers, $N_c(t = \infty)$, shown in Figure 6, are also in agreement with typical experimental data (10^{16}–10^{18} particles dm^{-3}).

Figure 6 shows a plot of the *total* particle number, $N_t = \sum_{j=1,\infty} v_j$, and the number of latex particles, $N_c(t)$, as a function of time. It can be seen that $N_t(t)$ can show a maximum at early times. $N_c(t)$, on the other hand, shows no maximum, and N_c and N_t will coincide at sufficiently long times, as all particles become large enough to be latex particles.

Note that although in the present treatment we have adopted the crude assumption that $g(t)$ is a simple step function, this could be improved by using the theory of Hansen and Ugelstad[1] and Fitch and Tsai,[8] who provide more complete descriptions of the "primary particle" stage of nucleation.

Comparison with PSD Data

We have shown above that physically realistic values of the various parameters can give time dependences of dN_c/dt and values of the final particle number which are in general agreement with experimental observation. Now, as pointed out above, a quantitative comparison of the coagulative nucleation model with experiment is not particularly meaningful, because of the number of adjustable parameters (r, J, W_{11}, and m) in the model whose precise values cannot be estimated a priori because of the well-known limitations of the DLVO theory. Nevertheless, it is clearly important to establish that values of these parameters within the physically reasonable range can quantitatively reproduce the most sensitive experimental data, viz., the time evolution of the PSD. It will be recalled that it is the treatment of these data that yields the results for the time evolution of dN_c/dt, which in turn provides convincing evidence for the correctness of the coagulative nucleation mechanism. It is also opportune here to point out that the original determination of dN_c/dt from the PSD[12] assumed that nucleation ceased abruptly after the attainment of the maximum (i.e., after the monotonic increase which is the important feature of dN_c/dt), whereas the model given in the preceding section shows that cessation should be comparatively rapid (after all surfactant has been used up). While stochastic broadening of the PSD would result in the PSD after nucleation being insensitive to such finer details of the time dependence of dN_c/dt, it is useful to check that this is indeed so. It is also useful to derive a relation which enables experimental PSDs to be readily interconverted with dN_c/dt. To accomplish this, we derive an expression for the time evolution of the PSD for a system where dN_c/dt is obtained from the full coagulative nucleation mechanism of the preceding section.

The general expression for the time evolution of the PSD is given by[27]

$$\frac{\partial \mathbf{n}}{\partial t} = \mathbf{\Omega n} - \frac{\partial}{\partial V}(\mathbf{Kn}) + \mathbf{c} \tag{17}$$

Here, $\mathbf{n}(V,t)$ is a vector with elements $n_i(V,t)$, which are relative number densities of latex particles of unswollen volume V containing i free radicals ($i = 0, 1, 2, ...$); $\mathbf{\Omega}$ is a matrix whose elements $\Omega_{ij}(V,t)$ describe the kinetic coupling between n_i and n_j (e.g., by the entry or exit of a free radical), $\mathbf{K}$ is a diagonal matrix whose nonzero elements $K_{ii}(V,t)$ give the rate of volume growth of a particle containing i free radicals, and $\mathbf{c}(V,t)$ is a vector whose elements $c_i(V,t)$ give the rate of creation of particles containing i free radicals at volume V. The PSD, $n(V,t)$, is then given by

$$n(V,t) = \sum_{i=0}^{\infty} n_i(V,t)$$

Certain simplifications can be made immediately to eq 17 for the case of interest, viz., interval I and early in interval II (interval I refers to when the particle number increases, and interval II to when it remains constant). During this period, we assume that no particle contains more than one free radical. This assumption is certainly valid for intervals I and II for monomers such as styrene, vinyl acetate, and methyl methacrylate, as long as the unswollen particle radius is not too large (say, greater than 80 nm for styrene), and should hold for most monomers during all of interval I and sufficiently early in interval II. One then only needs to consider n_0 and n_1; the Ω_{ij} then take a particularly simple form. One has also $K_{00} = 0$, $K_{11} = K = M_0 k_p C_m/(N_A d_p)$. Finally, the form for $\mathbf{c}$ [$\equiv(c_0,c_1)$] can be deduced as follows. Latex particles when newly formed can be assumed to contain a growing free radical: $c_0 = 0$; moreover, if one were to adopt the more reasonable assumption that (because of coagulation resulting in bimolecular termination[24]) newly formed latex particles may contain zero or one free radical with comparable probabilities, it is found[27,28] that subsequent free radical entry, exit, and bimolecular combination renders the PSD (at times sufficiently long after nucleation to be in interval II) insensitive to the initial ratio of c_0/c_1. One then has $c_1(t) \propto dN_c/dt$. The proportionality constant is found from the normalization. If one defines the n_i to be normalized so that

$$\sum_i \int_0^{\infty} n_i(V, t = \infty)\, dV = 1 \tag{18}$$

then one has

$$c_1(V,t) = \delta(V)\frac{dN_c(t)}{dt} \Big/ N_c(t = \infty) \tag{19}$$

Note that (through the Dirac δ function) this relation assumes that particles are created at volumes considerably less than the smallest particle observed in the electron microscopic PSD (at the start of interval II). Now, model calculations show that (for example) assuming that particles appear with a radius of 5 nm rather than zero radius

does not lead to any significant alteration in the computed PSD at the start of interval II. It is crucial to our development that one of the most important and sensitive experimental observables (the early-time PSD) is thus seen to be sensitive to the rate of particle formation but not the volume at which they appear (as long as this volume is acceptably small). This provides ample justification of the approximation of ignoring particle growth by propagation in the theoretical development of the previous section.

The elements of Ω are simplified with the assumption that no particle contains more than one free radical and that entry into a particle already containing a growing chain causes instantaneous termination (an accurate approximation for styrene and many other systems). Equation 17 then takes the form

$$\frac{\partial n_0}{\partial t} = -\rho n_0 + (\rho + k)n_1 \tag{20}$$

$$\frac{\partial n_1}{\partial t} = \rho n_0 - (\rho + k)n_1 - K\frac{\partial n_1}{\partial V} + c_1(V,t) \tag{21}$$

Here, ρ is the overall first-order rate coefficient for entry of free radicals (including effects of any reentry and heterotermination in the aqueous phase[26]) and k is the first-order rate coefficient for exit (desorption) of free radicals from the latex particles. Note that bimolecular termination within the latex particles does not appear in eq 20 and 21, since it is not a rate-determining step: it is so rapid that entry of a free radical into a latex particle which already contains a free radical results in essentially instantaneous termination.

In general, ρ and k may depend on V and also on time in quite a complex fashion if reentry and heterotermination are considered;[26] indeed the time dependence of ρ so resulting renders the equations nonlinear. Under such circumstances it is necessary to solve them numerically, comparatively efficient means for this being available.[28] However, analytic solutions can be obtained if certain assumptions (which are not particularly restrictive) are adopted.

To obtain analytic solutions, we first assume that ρ and k are independent of both V and t. Now, appropriate kinetic experiments[23,26] show, for example, that the V dependence of k can be quite pronounced ($k \propto V^{-2/3}$); however, PSD data on a single system alone (i.e., in the absence of kinetic data on a range of systems) are insufficient to distinguish any V dependence of ρ and k. Thus the values for ρ and k obtained from PSD data under this assumption will be averages of the true values over V and t. If necessary (and if additional appropriate kinetic data are available) such average values could then be refined by using a full numerical solution; the advantages of first obtaining these average values from the data using analytic solutions are obvious.

The second approximation used to obtain analytic solutions to eq 20 and 21 is to replace the functional form for $c_1(t)$ given by eq 19 and the theory of the preceding section by a simpler one, namely, by two straight lines as shown in Figure 7. Specifically, we write

$$dN_c/dt = u(t_0 - t)(t_1 + s_1 t) + T(t_0,t_2,t)(t_3 + s_3 t) \tag{22}$$

Here, $u(t_0 - t)$ and $T(t_0,t_2,t)$ are respectively the unit step function and top hat function:

$$\begin{aligned} u(t_0 - t) &= 1, \quad t \le t_0 \\ &= 0, \quad t > t_0 \end{aligned} \tag{23}$$

$$\begin{aligned} T(t_0,t_2,t) &= 1, \quad t_0 \le t \le t_2 \\ &= 0 \text{ otherwise} \end{aligned} \tag{24}$$

This simplification of $c_1(t)$ introduces negligible error in the final PSD, as long as the constants t_0, t_1, t_2, t_3, s_1, and s_3 are chosen to closely mimic the width and height of the proper numerical solution of eq 7–9. Note that the constraints of continuity, etc., fix the following relations: $t_1 + s_1 t_0 = t_3 t_0$, $t_3 + s_3 t_2 = 0$. In addition, if N_m° is the maximum value of dN_c/dt, computed from eq 7–9, one has also $N_m^\circ = t_1 + s_1 t_0 = t_3 + s_3 t_0$, and $t_0 = t_{max}$, where t_{max} is the value of t at which this maximum occurs. Thus only one parameter (say s_3) needs to be chosen to match a given $c_1(t)$ curve.

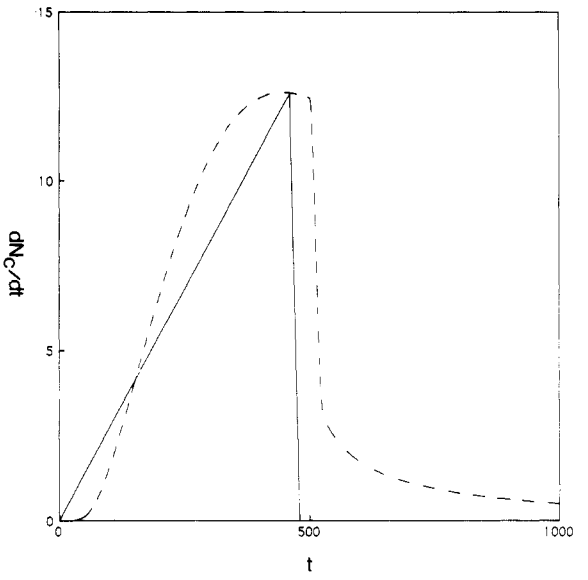

Figure 7. dN_c/dt (particles/10^{-14} dm^3 s^{-1}) which best fits data of Figure 8 as a function of time, t (s), for parameters as given for Figure 5. Full line: triangular function of eq 22; broken line: solution of eq 7–9 and 14–16.

Given eq 22, eq 20 and 21 can be readily (if somewhat tediously) solved by Laplace transforms. The final result, which appears as a complicated expression involving single and double integrals, is given in Appendix A. Despite their complexity, these expressions can be evaluated numerically with trivial computational time, using Gaussian quadrature for the single integrals and double application of Gaussian quadrature for the double integrals.

The expressions for $n_0(V,t)$, $n_1(V,t)$, and $n = n_0 + n_1$ given in Appendix A are valid for both intervals I and II, i.e., both during formation by coagulation and after nucleation has ceased, monomer droplets still being present so that C_m remains constant. Computationally, however, it is found to be preferable to use an alternative expression in interval II, since numerical evaluation of the multiple integrals is found to be quite time-consuming for values of t considerably greater than that for which nucleation has essentially ceased, $t = t_{I/II}$. It was found to be more convenient for computational purposes in interval II to use the solution to eq 20 and 21 given by Fourier transform with $dN_c/dt = 0$, the initial conditions at $t = t_{I/II}$ being given by the expression in Appendix A. The Fourier transform solution, for arbitrary initial conditions, is given in Appendix B; note that this replaces that given previously,[29] which was for more restricted initial conditions (as well as correcting some misprints in that reference). Numerical evaluation of the expression in Appendix B is conveniently and rapidly effected by using the fast Fourier transform algorithm.

Figure 1 shows the particle size distribution computed by these methods (full line) with parameters chosen to closely fit experimental data[12] (points). The data are for styrene at 50 °C, with [I] = 1.54×10^{-2} mol dm^{-3} $K_2S_2O_8$ and [S] = 3.38×10^{-2} mol dm^{-3} SDS. The values of ρ (=2.7

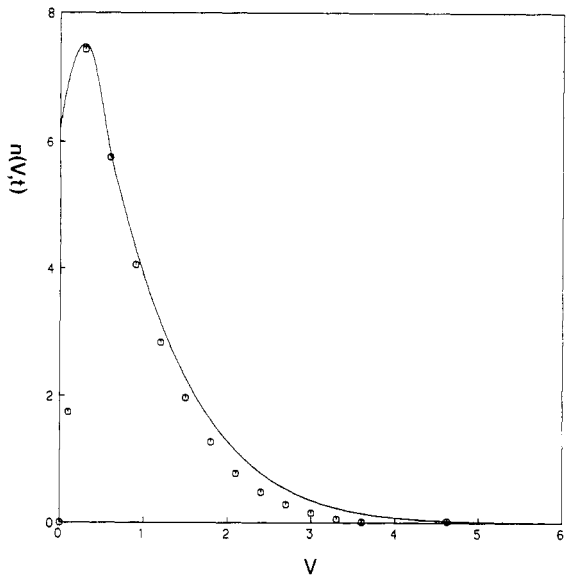

Figure 8. PSD, $n(V,t)$ [arbitrary units], as a function of volume V ($nm^3/10^4$), computed for monotonically increasing dN_c/dt with instantaneous cutoff at $t = 5$ min (full line) compared with second set of experimental data (points).

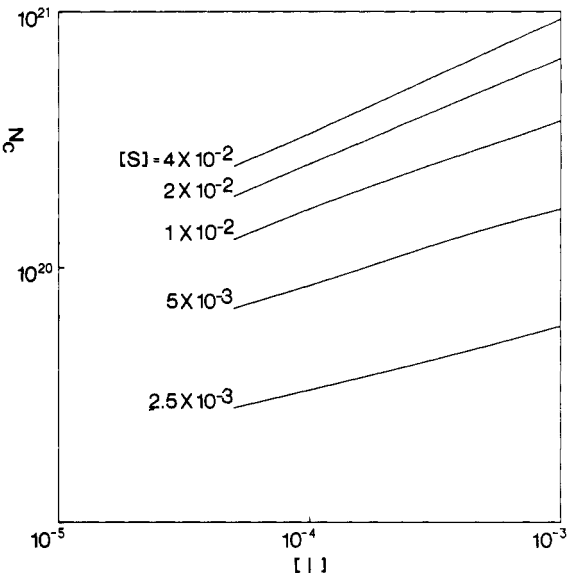

Figure 9. Dependence of final particle number, $N_c(t = \infty)$ [particles m^{-3}], on initiator concentration, [I] (mol dm^{-3}), for various surfactant concentrations, [S] (mol dm^{-3}), from eq 7–9 and 14–16; parameters are otherwise those for Figure 5.

$\times 10^{-3}$ s^{-1}), k (=3.0 $\times 10^{-3}$ s^{-1}), and K (=220 nm^3 s^{-1}) were chosen to reproduce both the kinetics and the evolution of the PSD from the first measurement (at $t = 8$ min, near the start of interval II to the second (at $t = 18$ min, much later in interval II). Note that the value of K is in accord with that computed from the expression $K = k_p C_m M_0 / N_A d_p$, using $k_p = 260$ dm^3 mol^{-1} s^{-1} and $C_m = 5.1$ mol dm^{-3} (yielding $K = 220$ nm^3 s^{-1}); these values for k_p and C_m are those determined from accurate kinetic studies of similar styrene systems.[23] The values of the coagulative nucleation parameters used to obtain Figure 7 are $r_1 = 4$ nm, $J = 2.0$ nm^{-1}, $W_{11} = 8 \times 10^3$, and $m = 10$; these are within the physically acceptable limits for this system, as given in the preceding section. The "feeding rate" $g(t)$ was taken to have the constant value of 10^{16} particles dm^{-3} s^{-1}, which is some 3 times the value calculated from the initiator concentration and decomposition rate. This effect is probably caused by the surfactant, SDS, acting as a chain-transfer agent; however, this postulate will be investigated in the future.

Another experiment, with similar conditions to that presented previously[8] (styrene at 50 °C, with [I] = 1.0 $\times$ 10^{-3} mol dm^{-3} $K_2S_2O_8$ and [S] = 3.50 $\times$ 10^{-2} mol dm^{-3} SDS), was performed and a PSD determined during interval I (at ca. 6% conversion and $t = 5$ min). This PSD (points) and that computed to give the best fit (full line) are shown in Figure 8. Again the parameters ρ (=4.4 $\times$ 10^{-3} s^{-1}), k (=1.9 $\times$ 10^{-2} s^{-1}), and K (=220 nm^3 s^{-1}) were chosen to closely reproduce both kinetics and the PSD. The same coagulation nucleation parameters for r_1, J, W_{11}, and m as found previously were found to reproduce the dN_c/dt vs. time graph obtained for this experiment. Since the PSD was derived during nucleation, there was no effect due to surfactant exhaustion, so the dN_c/dt vs. time graph was a simple monotonically increasing function with an instantaneous cutoff at $t = 5$ min (the time at which the PSD was determined).

It can be seen that these parameters give a time evolution of the PSD which is in good quantitative agreement with experiment. In particular, the observed positive skewness of the PSD at early times (which is a strong indicator of a coagulative nucleation mechanism) is well reproduced. The observed final particle number (5.1 $\times$ 10^{17} dm^{-3}) is also reproduced to within 15%.

Although the form of dN_c/dt given in eq 22 is employed because it provides a suitable fit to the form of the nucleation rate given in the preceding section, it can in fact be used as well to mimic a number of quite different situations by suitable choices of parameters. Thus, for example, one can have a dN_c/dt which is a monotonically decreasing function of time or which is independent of time. As found by Lichti et al.[12] using numerical solutions (with V-dependent ρ and k), such forms of dN_c/dt cannot give rise to an interval II PSD which shows positive skewness (at least for physically reasonable volume dependences of ρ and k).

Dependence on [I] and [S]

One of the commoner pieces of evidence used to infer a nucleation mechanism is the dependence of final particle number (or alternatively maximum polymerization rate, in an ab initio system) on initiator or surfactant concentrations, the simple micellar entry and homogeneous nucleation theories[10,11] leading to

$$N_c(t = \infty) \propto [I]^{2/5}[S]^{3/5} \tag{25}$$

It is clearly of interest to examine the predictions of the present coagulative nucleation model and to compare both with eq 25 and experiment. Figures 9 and 10 show $N_c(t = \infty)$ computed from eq 7–9, 14, and 15 as functions of [I] and [S]. In these computations, the parameter κ was kept constant for [S] greater than the cmc and computed from the relation

$$\kappa = \left(\frac{2e^2 N_A \gamma z^2}{\epsilon k_B T} \right)^{1/2} \tag{26}$$

where γ is the ionic strength at the cmc, e is the charge on the electron, z is the valence, and ϵ the permittivity. The following calculations were confined to surfactant concentrations at or above the cmc, since the applicability of the DLVO formulation used here to surfactant concentrations below the cmc is questionable. In these calculations, r_1 was taken to be 4 nm, $\psi_0 = 200$ mV, $J = 2$ nm^{-1}, $m = 10$, and $W_{11} = 8 \times 10^3$. The dependence of $N_c(t = \infty)$ on [I] above the cmc is shown in Figure 9; this dependence can be approximated by

$$N_c(t = \infty) \propto [I]^{0.4} \tag{27}$$

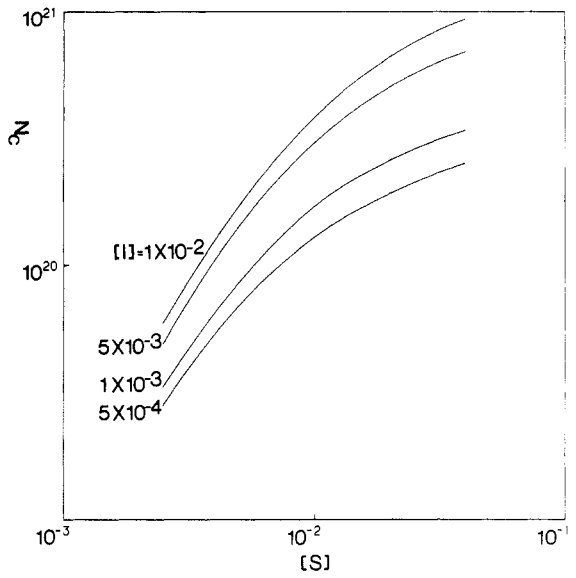

Figure 10. Dependence of final particle number, $N_c(t = \infty)$ [particles m^{-3}], on surfactant concentration, [S] (mol dm^{-3}), for various initiator concentrations, [I] (mol dm^{-3}), from eq 7–9 and 14–16; parameters are otherwise those for Figure 5.

This is in accord with the classical prediction of Smith and Ewart.[10]

For fixed [I], the $N_c(t = \infty)$ increases with [S] but with a monotonically diminishing exponent, as shown in Figure 10. The slope of $d(\log N_c)/d(\log t)$ varies in the range 0.4–1.2. One notices immediately that the simple form of eq 25 is thus seen to be encompassed within the coagulative nucleation theory.

The experimental observation[11] that the exponent of [S] decreases with increasing [S] can be explained by the coagulative nucleation mechanism. At high [S], the nucleation time will be long in duration since the new precursor particles will be readily stabilized. As a result, more latex particles will be formed and eventually will outnumber the very small precursor particles at long times. Thus precursor/latex particle collisions will become more and more frequent and fewer latex particles will be formed. The dN_c/dt will approach zero at these long times and N_c will approach a constant. This effect, that N_c approaches a constant at high [S], is seen experimentally.[11,30] It should be noted that the exponent predicted by Smith and Ewart, 0.6, is constant over all [S] and fails to predict the high-[S] effects observed experimentally.

Clearly, a more quantitative comparison of experimental dependences of $N_c(t = \infty)$ (and of the time dependence of dN_c/dt) on [I] and [S] is a fruitful field for future work. An obvious preliminary conclusion is that the complex behavior seen in experiment can readily be explained by the theory.

It has been shown in the present paper that the coagulative nucleation theory can quantitatively fit data on the time dependence of the nucleation rate and particle number for styrene systems. Its general predictions are also in agreement with results on particle formation in emulsion systems. Coagulative nucleation may well be a widespread mechanism for particle formation in these systems; the present paper provides means for quantitatively testing this postulate by comparison with experiment.

Acknowledgment. The assistance of Mr. B. Whang in obtaining data and the collaboration of the Sydney University Electron Microscope unit are gratefully acknowledged, as are the support of a Commonwealth Postgraduate Research Award for P.J.F., the financial support of the Australian Research Grants Scheme, and the comments of anonymous referees which led to significant improvement in the manuscript.

Appendix A

Equations 19–22 are solved by Laplace transform to yield

$$n_0 = \frac{q}{K}e^{-qM}\int_0^t\Big[t_1f(\tau) - (t_1 + s_1t_0 - t_3 - s_3t_0)f(\tau - t_0) - (t_3 + s_3t_2)f(\tau - t_2) + \Big[\int_0^\tau\{s_1f(\lambda) + (s_3 - s_1)f(\lambda - t_0) - s_3f(\lambda - t_2)\}\,d\lambda\Big]\,d\tau\Big]$$

$$n_1 = \frac{1}{K}e^{-qM}[t_1f(t) - (t_1 + s_1t_0 - t_3 - s_3t_0)f(t - t_0) - (t_3 + s_3t_2)f(t - t_2) + \int_0^t\{(s_1 + t_1\rho)f(\tau) - [\rho(t_1 + s_1t_0 - t_3 - s_3t_0) + s_1 - s_3]f(\tau - t_0) - [\rho(t_3 + s_3t_2) + s_3]f(\tau - t_2) + \rho\int_0^\tau[s_1f(\lambda) - (s_1 - s_3)f(\lambda - t_0) - s_3f(\lambda - t_2)]\,d\lambda\}\,d\tau]$$

where $f(x) = u(x - M)\exp[-\rho(x - M)]I_0[\{4M\rho q(x - M)\}^{1/2}]$, I_0 being a modified Bessel function, $q = \rho + k$, and $M = V/K$.

Appendix B

In interval II (i.e., $g = 0$), eq 20 and 21 yield the following expressions for the Fourier transforms of n_0 and n_1:

$$F_j = \int_{-\infty}^{\infty}\exp(-2\pi isV)n_j(V,t)\,dV, \qquad j = 0, 1$$

$$= A_j^+\exp(\lambda_+t) + A_j^-\exp(\lambda_-t)$$

$$\lambda_\pm = -\tfrac{1}{2}(\rho + k + 2\pi isK) \pm \tfrac{1}{2}\Delta$$

$$\Delta = [(\rho + q + 2\pi isK)^2 - 8\rho\pi isK]^{1/2}$$

$$A_0^\pm = [qF_1(0) - (\rho + \lambda_\pm)F_0(0)]/(\lambda_\pm - \lambda_\mp)$$

$$A_1^\pm = [\rho F_0(0) + (\rho + \lambda_\pm)F_1(0)]/(\lambda_\pm - \lambda_\mp)$$

where $F_i(0)$ is the Fourier transform of $n_i(V,t = 0)$. The values of n_i are determined from F_i by the fast Fourier transform algorithm.

References and Notes

(1) Hansen, F. K.; Ugelstad, J. In "Emulsion Polymerization"; Piirma, I., Ed.; Academic Press: New York, 1982.
(2) Eliseeva, V. I. *Acta Polym.* **1981**, *32*, 355.
(3) Harkins, W. D. *J. Chem. Phys.* **1945**, *13*, 381.
(4) Priest, W. J. *J. Phys. Chem.* **1952**, *56*, 1077.
(5) (a) Sujkov, A. V.; Grizkova, I. A.; Medvedev, S. S. *Kolloid Z.* **1972**, *34*, 203. (b) Ugelstad, J.; El-Aasser, M. S.; Vanderhoff, J. W. *J. Polym. Sci., Polym. Lett. Ed.* **1973**, *11*, 503.
(6) Eliseeva, V. I.; Sarkova, N. T.; Jerks, E. I. *Vysokomol. Soedin., Ser. A* **1967**, *9*, 2478.
(7) Fitch, R. M.; Tsai, C. H. In "Polymer Colloids"; Fitch, R. M., Ed.; Plenum Press: New York, 1971.
(8) Fitch, R. M. In "Emulsion Polymers and Emulsion Polymerization"; Basset, D. R., Hamielec, A. E., Eds.; American Chemical Society: Washington, D.C., 1981; ACS Symp. Ser.
(9) Fitch, R. M.; Watson, R. C. *J. Colloid Interface Sci.* **1979**, *68*, 14.
(10) Smith, W. V.; Ewart, R. H. *J. Chem. Phys.* **1948**, *16*, 592.
(11) Roe, C. P. *Ind. Eng. Chem.* **1968**, *60*, 20.
(12) Lichti, G.; Gilbert, R. G.; Napper, D. H. *J. Polym. Sci., Polym. Chem. Ed.* **1983**, *21*, 269.
(13) Morton, M.; Kaiserman, S.; Altier, M. *J. Colloid Sci.* **1954**, *9*, 300.
(14) Hawkett, B. S.; Napper, D. H.; Gilbert, R. G. *J. Chem. Soc., Faraday Trans. 1* **1980**, *76*, 1323.
(15) von Smoluchowski, M. *Phys. Z.* **1916**, *17*, 557.

(16) Overbeek, J. Th. G. In "Colloid Science"; Kruyt, H. R., Ed.; Elsevier: Amsterdam, 1960.
(17) Müller, H. *Kolloid.-Beih.* **1928**, *26*, 257.
(18) Krumrine, P. R.; Vanderhoff, J. W. In "Polymer Colloids"; Fitch, R. M., Ed.; Plenum Press: New York, 1980; p 289; Vol. II.
(19) (a) Aoyagi, T. Ph.D. Thesis, University of Connecticut, 1981. (b) Aoyagi, T.; Fitch, R. M., to be published.
(20) Hunter, R. J. "The Zeta Potential in Colloid Science"; Academic Press: London, 1981.
(21) Dunn, A. S.; Chong, L. C. H. *Br. Polym. J.* **1970**, *2*, 49.
(22) Hansen, F. K.; Ugelstad, J. *J. Polym. Sci., Polym. Chem. Ed.* **1979**, *17*, 3047.
(23) Hawkett, B. S.; Gilbert, R. G.; Napper, D. H. *J. Chem. Soc., Faraday Trans. 1* **1980**, *76*, 1323.
(24) Adams, M. E.; Whang, B. C. Y.; Gilbert, R. G.; Napper, D. H., to be published.
(25) Hiemenz, P. C. "Principles of Colloid and Surface Chemistry"; Marcel Dekker: New York, 1977; p 369.
(26) Gilbert, R. G.; Napper, D. H. *J. Macromol. Sci., Rev. Macromol. Chem.* **1983**, *C23*, 127.
(27) Lichti, G.; Gilbert, R. G.; Napper, D. H. In "Emulsion Polymerization"; Piirma, I., Ed.; Academic Press: New York, 1982.
(28) Lichti, G.; Hawkett, B. S.; Napper, D. H.; Gilbert, R. G.; Sangster, D. F. *J. Polym. Sci., Polym. Chem. Ed.* **1981**, *19*, 925.
(29) Lichti, G.; Gilbert, R. G.; Napper, D. H. *J. Polym. Sci., Polym. Chem. Ed.* **1977**, *15*, 1957.
(30) Sutterlin, N. In "Polymer Colloids"; Fitch, R. M., Ed.; Plenum Press: New York, 1980; Vol. II, p 583.

Synthesis of a Two-Dimensional Array of Organic Functional Groups: Surface-Selective Modification of Poly(vinylidene fluoride)

Anthony J. Dias and Thomas J. McCarthy*

Polymer Science and Engineering Department, University of Massachusetts, Amherst, Massachusetts 01003. *Received May 24, 1984*

ABSTRACT: An autoinhibitive surface modification reaction of poly(vinylidene fluoride) has been developed and assayed for surface selectivity. Phase-transfer-catalyzed dehydrofluorination using aqueous sodium hydroxide and tetrabutylammonium bromide produces an eliminated surface. Contact angle, ESCA, ATR IR, gravimetric, UV–vis, and SEM analyses indicate a mild, surface-selective reaction. Estimates of reaction depth are ~10 Å or less. The basis for the surface selectivity of this reaction is the product inhibition of the phase transport step.

Introduction

The chemical environment of reactive portions of organic molecules (functional groups) is markedly affected by the state of the organic material. Functional group environments in gases, liquids, and solids have obvious differences. In solution (the condition under which most organic reactions are carried out), functional groups are surrounded by solvent molecules. Forces due to solvation are often responsible for the outcomes and rates of chemical reactions. Solution organic chemistry has developed to an advanced stage.

The extent to which this body of knowledge can be applied to functional groups on polymer surfaces is not obvious. The chemical environment of surface functional groups is certainly different: if the solid polymer is placed in a nonswelling liquid, the environment of the surface functional groups is that of a solid in one direction and that of a solution in the other. Forces due to solvation are attenuated. If the solid is placed in contact with a vapor, its environment is half solid-like, half gas-like. Geometrical constraints on functional groups confined to two dimensions should inhibit reactivity: organic chemistry requires three dimensions. Surface physics should perturb reactivity as well: polymers tend to concentrate nonpolar functionality at their surfaces to minimize surface energy;[1-4] hence surface reactions with polar transition states may have especially high activation barriers.

To study the organic chemistry of surface-confined polymer functional groups, particularly with regard to how their two-dimensional environment affects reactivity, refined methods for the introduction of polar functionality onto chemically resistant nonpolar solid organic polymers must be developed. The requisite substrate for approaching this objective is a two-dimensional array of versatile organic functional groups covalently attached to a polymer which is not swollen by a variety of solvents and is inert to the reaction conditions for a variety of functional group transformations. Presently available techniques for polymer surface modification are not appropriate for preparation of this substrate: oxidation,[4-6] reduction,[7] flame treatment,[8] and corona discharge treatment[9] all involve severe conditions and products of these reactions are less inert than the unmodified polymer; hence autocatalysis and pitting ensue (Figure 1). The cascade of secondary reactions makes control of surface functionality difficult if not impossible.

Here we report an *autoinhibitive* surface modification reaction of poly(vinylidene fluoride) (PVDF) which, as expected from the modification kinetics allows surface-selective functional group introduction. The depth of reaction is estimated by several techniques.

Experimental Section

Materials. Poly(vinylidene fluoride) films were 5-mil Pennwalt Kynar obtained from Westlake Plastics. The samples were uniformly 1.27×10^{-2} cm thick and had a density of 1.74 g/cm^3. Films were extracted in refluxing dichloromethane (30 min) and dried in a vacuum oven (14 h, 50 °C, 0.05 mm) to constant mass. This procedure consistently produced films which were free from contaminants that interfere with surface characterization. All water was distilled twice. Sodium hydroxide solution (8 N) was stored in polypropylene screw-cap bottles to restrict silicate presence. Bromine in carbon tetrachloride (0.2 N) was kept in an amber-colored bottle in a refrigerator. Dimethylformamide was distilled from barium oxide at 39 mm (76 °C) and stored under nitrogen.

Methods. Advancing and receding contact angles were obtained by using water distilled from potassium permanganate, a Rame–Hart telescopic goniometer, and a Gilmont syringe. The reported data are the mean of at least six measurements and their

0024-9297/84/2217-2529$01.50/0